

Power Analysis of a Multimodular Wind Power System Including PMG, Active Rectifier and VSI

Sergey Kharitonov, Sergey Brovanov, Gennady Zinoviev
Novosibirsk State Technical University
kharit1@yandex.ru

Abstract - This paper is concerned with the power characteristics of the wind power system based on modular principle. A mathematical model for analysis of energy characteristics of the electric power generation system consisting of a synchronous generator with excitation from permanent magnets, the active rectifier and the voltage inverter with PWM is considered. Various algorithms to control the active rectifier and inverter for variable speed wind turbine shaft are analyzed. Analytical relations for the calculation of currents, voltages and power generation in the system are obtained. Recommendations on the choice of control algorithms and structural circuits of the generation electrical energy at a variable speed of shaft of wind turbine (WT) are given.

Index Terms -- permanent magnet synchronous, active rectifier, voltage-source inverter, power characteristics.

I. INTRODUCTION

A promising energy conversion system for the Wind Power Installations (WPI) with variable wind turbine speed is the system "Permanent Magnet Synchronous generator – Active Rectifier – Voltage Source Inverter" [1], Fig.1. Further the system is called Wind Power Generation System (WPGS).

WPGS-type systems can realize all the required options: generation mode with non-linear load, asymmetrical and non-stationary load, electric starter launch mode, in-phase and parallel work with electrical network and other WPI.

This paper evaluates general power characteristics of the system in S_G , S_R , S_I , S_T sections in condition of working for high power network. The main feature of this research is taking into account factors appearing due to variable speed of the wind turbine shaft. These factors are variable frequency and magnitude of the synchronous generator (G) output voltage and dependency of the generated power on wind turbine rotation frequency. Besides that, presence of the active rectifier (R) changes functional and energetic abilities of the WPGS.

II. MAIN POWER CHARACTERISTICS OF THE SYSTEM "SYNCHRONOUS GENERATOR – ACTIVE RECTIFIER"

Power characteristics of electromagnetic processes in WPGS define the efficiency of the mechanical energy conversion of shaft rotating with variable speed into electrical energy by synchronous generator and voltage source inverters. Also these characteristics evaluate degree of the WPGS influence on electrical network through its energy quality performance.

The main power characteristics are efficiency, power factor and THD. These characteristics are indirect because they require calculation of the RMS values for currents and voltages.

For the further analysis the following quantities have been chosen, as basic:

$$\begin{aligned} U_{dc} &= \sqrt{3}U_{N'}; E_b = U_{dc}/\sqrt{3} = U_{N'}; \omega_b = E_b/\Psi_o; \\ X_b &= \omega_b(L_f + L_d); I_b = I_{sc} = E_b/X_b; S_b = 3E_b I_b/2, \end{aligned} \quad (1)$$

where $U_{N'}$ – is the magnitude of the electric network voltage reduced to the primary transformer winding, T , $\Psi_o = const$ – is the magnetic linkage generated by permanent magnets.

Let us denote $q = L_f/L_d$ and $k_L = L_q/L_d$ then taking into account (1) it can be written:

$$\begin{aligned} X_{fR}^* &= \omega^* q/(1+q), X_d^* = \omega^*/(1+q), \\ X_q^* &= \omega^* k_L/(1+q), X_{fR}^* = \omega^* q/(1+q), \\ X_d^* &= \omega^*/(1+q), X_q^* = \omega^* k_L/(1+q), \\ X_{d\Sigma}^* &= X_d^* + X_{fR}^* = \omega^* \\ X_{q\Sigma}^* &= X_q^* + X_{fR}^* = \omega^* (k_L + q)/(1+q). \end{aligned}$$

Let us assume, that the blank cycle EMF of the generator, e_{Gm}^* , and active rectifier control voltage are conformed to the following equations:

$$\begin{cases} e_{Gm}^* = \omega^* \cos[\vartheta - (m-1)2\pi/3]; \\ u_{Rcm}^* = u_c/u_{sc} \sin(\theta_m) = M \sin(\theta_m); \end{cases}$$

where

$$\begin{aligned} \theta_m &= \vartheta - (m-1)2\pi/3 + \pi/2 - \phi_{Rc}; \\ \vartheta &= \omega t; m = 1, 2, 3 (a, b, c); \end{aligned}$$

and u_c – is the amplitude of control input wave, u_{sc} – is the amplitude of sawtooth carrier wave, M – is the modulation index.

Neglecting by the active losses, equations of the "G-R" system in the rotating dq frame with angular location $\gamma(\vartheta) = \vartheta - \pi/2$ can be written as:

$$\begin{aligned} u_{rd}^* &= -\omega^* \frac{di_{Gd}^*}{d\vartheta} + \omega^* \frac{k_L + q}{1+q} \cdot i_{Gq}^*; \\ u_{rq}^* &= -\omega^* \frac{k_L + q}{1+q} \cdot \frac{di_{Gq}^*}{d\vartheta} - \omega^* i_{Gd}^* + \omega^*. \end{aligned} \quad (2)$$

Active (P), reactive (Q) and the total power (S) for the fundamental harmonic can be found through the following equations (here and further all fundamental components have index 0):

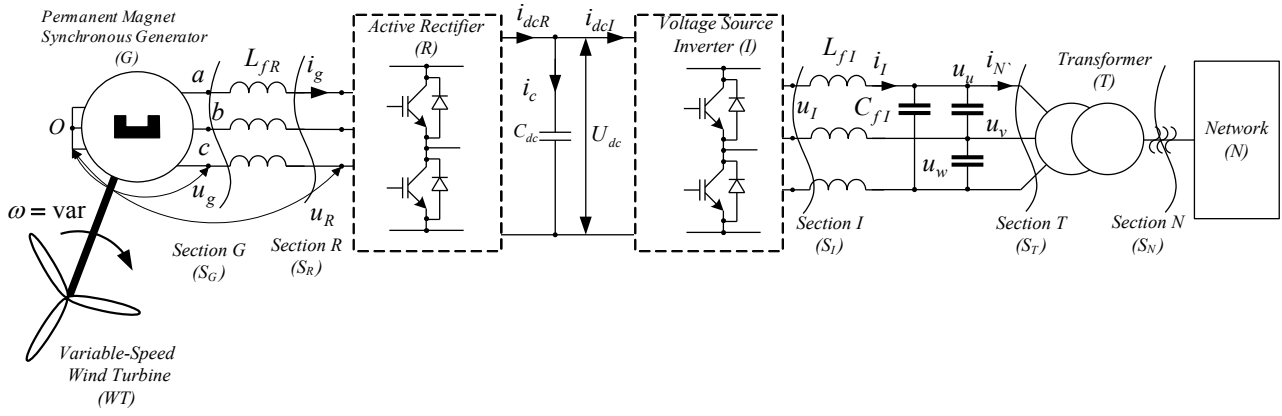


Fig. 1. Structure of the Wind Power Generation System.

$$\begin{cases} P_{SGo}^* = P_{SRo}^* = P_{SNo}^* = \omega^* i_{gqo}^* , \\ Q_{SGo}^* = u_{Gdo}^* i_{Gqo}^* - u_{Gqo}^* i_{Gdo}^* ; Q_{SRo}^* = u_{Rdo}^* i_{Gqo}^* - u_{Rqo}^* i_{Gdo}^* ; \\ S_{SGo}^* = \sqrt{(P_{SNo}^*)^2 + (Q_{SGo}^*)^2} ; S_{SRo}^* = \sqrt{(P_{SNo}^*)^2 + (Q_{SRo}^*)^2} ; \end{cases}$$

It has been taken into account that active power in each section is equal to the generated power for electric network.

Active power value is not changed with considering higher harmonics. Calculation of reactive and total power with considering higher harmonics is shown in [2]. Orthogonal components d and q are $M_d = M \sin \phi_{Rc}$ and $M_q = M \cos \phi_{Rc}$ respectively.

Taking into account high frequency ripples, equations for the active rectifier will be written as in (3) at the bottom of the page [2].

$$\begin{cases} u_{Rd}^* = u_{Rdo}^* + \Delta u_{Rd}^* ; u_{Rdo}^* = \sqrt{3} M \sin(\phi_{Rc}) / 2 = \sqrt{3} M_d / 2 ; \\ u_{Rq}^* = u_{Rqo}^* + \Delta u_{Rq}^* ; u_{Rqo}^* = \sqrt{3} M \cos(\phi_{Rc}) / 2 = \sqrt{3} M_q / 2 ; \end{cases} \quad (3)$$

In the equation (3) u_{Rdo}^* , u_{Rqo}^* – are the fundamental harmonic orthogonal components in the active rectifier, Δu_{Rd}^* , Δu_{Rq}^* – are the higher harmonic orthogonal components in the active rectifier, $J_p(x)$ – is the first order Bessel function, $a_R = \omega_{cr} / \omega$ – is the angular frequency of PWM in the active rectifier.

Analytical equations for generator currents were defined in [2]. Generator current and voltage can be defined by the similar way.

$$\begin{cases} i_{Gd}^* = i_{Gdo}^* + \Delta i_{Gd}^* ; i_{Gq}^* = i_{Gqo}^* + \Delta i_{Gq}^* \\ u_{Gd}^* = u_{Gdo}^* + \Delta u_{Gd}^* ; u_{Gq}^* = u_{Gqo}^* + \Delta u_{Gq}^* \end{cases}$$

For steady state condition it can be written:

$$i_{Gqo}^* = \frac{u_{Rdo}^*}{X_{q\Sigma}^*} = \frac{1+q}{\omega^* (k_L + q)} \cdot u_{Rdo}^* = \frac{\sqrt{3}}{2} \frac{1+q}{\omega^* (k_L + q)} M \sin(\phi_{Rc}) ;$$

$$i_{Gdo}^* = 1 - \frac{u_{Rqo}^*}{\omega^*} = 1 - \frac{\sqrt{3}}{2} \frac{1}{\omega^*} M \cos(\phi_{Rc}) ;$$

$$u_{Gdo}^* = u_{Rdo}^* - X_{Rf}^* i_{Gdo}^* = \frac{\sqrt{3}}{2} \frac{k_L}{k_L + q} M \sin \phi_{Rc} ;$$

$$u_{Gqo}^* = u_{Rqo}^* + X_{Rf}^* i_{Gqo}^* = \frac{1}{1+q} \left[\omega^* q + \frac{\sqrt{3}}{2} \frac{k_L}{k_L + q} M \cos \phi_{Rc} \right] .$$

RMS values for voltage and current of the active rectifier will be defined using results of [2] and well known relations:

$$\begin{cases} U_{R,rms} = \sqrt{M/2} ; v_{uR} = I_{R(1),rms} / U_{R,rms} = \sqrt{3M}/2 ; \\ I_{G,rms} = \sqrt{(i_{Gdo}^*)^2 + (i_{Gqo}^*)^2 + (\Delta I_G^*)^2} / \sqrt{2} , \end{cases}$$

where

$$\begin{cases} \Delta I_G^* \approx \left(\frac{\sqrt{6}}{\pi \cdot \omega^*} \right) \cdot \left(J_1(\pi \cdot M)^2 \frac{a_R^2 + 1}{(a_R + 1)^2 (a_R - 1)^2} \right)^{\frac{1}{2}} ; \\ v_{iG} = \sqrt{(i_{Gdo}^*)^2 + (i_{Gqo}^*)^2} / I_{G,rms} . \end{cases}$$

RMS value of the generator voltage will be defined assuming $k_L \rightarrow 1$:

$$U_{G,rms} = \frac{1}{\sqrt{2}} \sqrt{(\omega^* \cos \theta)^2 + \frac{1}{(1+q)^2} \cdot \left[M - \left(\frac{\sqrt{3}}{2} M \cos \phi_{Rc} \right)^2 \right]} ,$$

where θ – is the angle between the fundamental harmonics of the generator EMF and the generator voltage, Fig. 2, defining as $\theta = \arctg u_{Gdo}^* / u_{Gqo}^*$.

The character of change of the generated power, voltages and currents will be considered further using previously derived equations. For WPI with variable speed of the wind turbine generated active power (P_{WT0}^*) in working speed range ($\omega^* \in \{\omega_{WT \min}^*, \omega_{WT \max}^*\}$) is defined by wind velocity and known turbine parameters.

Thus, generated active power can be found from equation (4)

$$P_{WT0}^* = \gamma \cdot (\omega^*)^3 \quad (4)$$

Where $\gamma = const$ – is a construction parameter. Without taking into account active losses $P_{Ro}^* \approx P_{WT0}^*$.

In the sections S_R and S_G q -components of the voltage with specified active power are defined by the following equations:

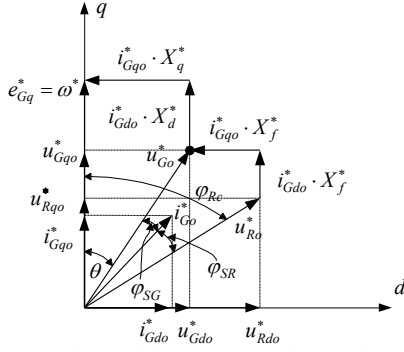


Fig. 2. Vector diagram of the Generator-Rectifier system in dq -frame.

$$u_{Rqo}^* = \omega^* \cdot \left(1 - \frac{P_{Ro}^*}{u_{Rdo}^*} \right) \frac{k_L + q}{k_L - 1};$$

$$u_{Gqo}^* = \omega^* \cdot \left(1 - \frac{P_{Ro}^*}{u_{Gdo}^* (1+q)} \right) \frac{k_L}{k_L - 1}.$$

Generated active power of the system can be found through the d -components of this voltage:

$$P_{Ro}^* = e_{Gq}^* i_{Gqo}^* = \omega^* i_{Gqo}^* = \omega^* \cdot u_{Rdo}^* / X_{q\Sigma}^* =$$

$$= \omega^* \cdot u_{Rdo}^* / X_q^* = u_{Rdo}^* \cdot (1+q) / (k_L + q) =$$

$$= u_{Gdo}^* \cdot (1+q) / k_L,$$

For $k_L \rightarrow 1$, $P_{Ro}^* \approx u_{Rdo}^* = (1+q)u_{Gdo}^*$. The total power and the displacement power factor in section S_R :

$S_{Ro}^* = \left[(Q_{Go}^*)^2 + (P_{Go}^*)^2 \right]^{1/2}$, $\cos \phi_R = P_{Ro}^* / S_{Ro}^*$, where the reactive power Q_{Ro}^* is defined by:

$$Q_{Ro}^* = \frac{1+q}{\omega^* (k_L + q)} (u_{Rdo}^*)^2 + \frac{1}{\omega^*} (u_{Rqo}^*)^2 - u_{Rqo}^*.$$

As can be seen from the Fig. 3, there are minimums of the total power for certain values of the angular frequency, when the reactive power is zero. Let us denote the frequency when the minimum total power as ω_0^* . This frequency is defined by:

$$\omega_0^* = u_{Rqo}^* + \frac{(u_{Rdo}^*)^2 (1+q)}{u_{Rqo}^* (1+k_L)} = u_{Gqo}^* + \frac{(u_{Gdo}^*)^2}{u_{Gqo}^* k_L}$$

From the equation for Q_{Ro}^* an equation linking coordinates of u_{Rdo}^* and u_{Rqo}^* can be obtained:

$$\left(u_{Rdo}^* / \gamma_Q R_Q \right)^2 + \left[(u_{Rqo}^* - \omega^* / 2) / R_Q \right]^2 = 1 \quad (5)$$

Where $\gamma_Q = \sqrt{(k_L + q) / (1+q)}$, $R_Q = \sqrt{\omega^* Q_{Ro}^* + (\omega^* / 2)^2}$. Equation (5) is the ellipse equation with the big axis is $2a_d$ and the small axis is $2b_q$, where $a_d = \gamma_Q R_Q$; $b_q = R_Q$. The ellipse center is located in coordinates $(0, \omega^* / 2)$. In the polar coordinates equation (5) will be following:

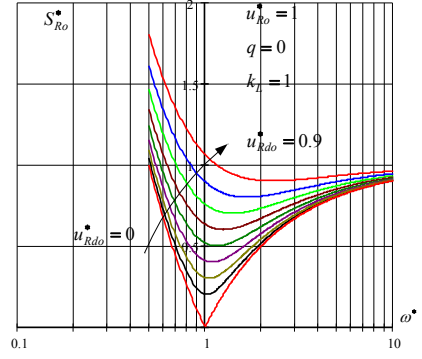


Fig. 3. Dependence S_R^* on ω^*

$$\rho(\varphi)^2 \cdot [1 - (\varepsilon \cos \varphi)^2] - 2\rho(\varphi)\rho_0 \left[\left(\frac{b_q}{a_d} \right)^2 \cos \varphi \cos \varphi_0 + \sin \varphi \sin \varphi_0 \right] +$$

$$+ \rho_0^2 \cdot [1 - (\varepsilon \cdot \cos \varphi_0)^2] - b_q^2 = 0,$$

where $\varphi \in (0, 2\pi)$, ρ_0 , φ_0 are the ellipse center coordinates and parameter ε is defined by the following equations:

$$\rho_0 = \omega^* / 2; \quad \phi_0 = \pi / 2; \quad \varepsilon^2 = 1 - (b_q / a_d)^2 = (k_L - 1) / (k_L + q).$$

Thus the locus equation $u_{Ro}^*(\varphi) = \sqrt{(u_{Rdo}^*)^2 + (u_{Rqo}^*)^2}$ in section S_R^* can be written:

$$u_{Ro}^*(\varphi) = \omega^* \sin \varphi + \frac{\sqrt{(\omega^* \sin \varphi)^2 + 4\omega^* Q_{Ro}^* (1 - \varepsilon^2 \cos^2 \varphi)}}{2(1 - \varepsilon^2 \cos^2 \varphi)}.$$

Locus $u_{Ro}^*(\varphi)$ for different values of ω^* and is shown on Fig. 5.

Here and further circle with the radius $u_{Ro \max}^* = \sqrt{3} / 2$ limits mode with $M = 1$ i.e. out of this circle the modulation index is limited. Therefore all obtained equations are correct within this circle.

Varying values of u_{Rdo}^* and u_{Rqo}^* makes it possible to regulate generated active power and consumed reactive power by the fundamental harmonic. Since $P_{Ro}^* \approx u_{Rdo}^*$, it can be seen from Fig. 5 that the maximum active power, which is defined by the maximum d -component of the locus, also considerably depends on reactive power (Q_{Ro}^*) and ω^* . What is more, with the negative value of Q_{Ro}^* value of $P_{Ro \max}^*$ decreases:

$$P_{Ro \max}^* \approx \gamma_Q R_Q \approx \sqrt{\omega^* Q_{Ro}^* + (\omega^* / 2)^2}$$

On conditions that $Q_{Ro}^* = \text{tg} \phi_{SR} P_{Ro}^*$ and $q = 0$ equation (5) can be rewritten:

$$\left(\frac{P_{Ro}^* - \frac{\omega^*}{2} \text{tg} \phi_{SR} \cdot k_L}{\sqrt{k_L} \cdot \frac{\omega^*}{2} \sqrt{1 + k_L (\text{tg} \phi_{SR})^2}} \right)^2 + \left(\frac{u_{Rqo}^* - \frac{\omega^*}{2}}{\frac{\omega^*}{2} \sqrt{1 + k_L (\text{tg} \phi_{SR})^2}} \right)^2 = 1 \quad (6)$$

$$a_d = \sqrt{k_L} \sqrt{1 + k_L (\text{tg} \phi_{SR})^2} \cdot \omega^* / 2; \quad b_q = \sqrt{1 + k_L (\text{tg} \phi_{SR})^2} \cdot \omega^* / 2.$$

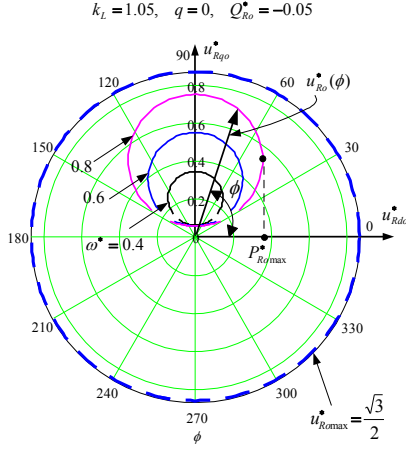


Fig. 4. Locus for $u_{Ro}^*(\phi)$

From this equation dependence $P_{Ro\max}^*$ on ϕ_{SR} can be obtained:

$$P_{Ro\max}^* = \sqrt{k_L} \cdot [\sqrt{k_L} \operatorname{tg} \phi_{SR} + \sqrt{1 + k_L (\operatorname{tg} \phi_{SR})^2}] \cdot \left(\frac{\omega^*}{2} \right)$$

Fig. 5 shows changing of $P_{Ro\max}^*$ ($P_{Ro\max(1)}^*$, $P_{Ro\max(2)}^*$, $P_{Ro\max(3)}^*$) with different values of ϕ_{SR} .

Thus, from the obtained results it can be concluded that there are operating modes with different values of $\cos(\phi_{SR})$ by varying ω^* . It became possible thanks to independent regulating of the orthogonal components of the reference vector u_{Ro} by the active rectifier. For instance, following modes are possible: fundamental harmonics of current and generator EMF are in-phase, Fig. 6, a; fundamental harmonics of current and generator voltage are in-phase, Fig. 6, b; fundamental harmonics of current and generator voltage are not in-phase and their phase difference varies.

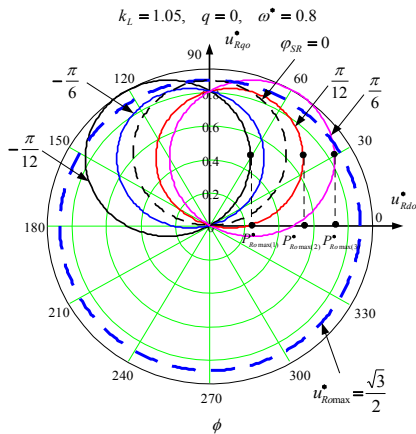


Fig. 5. Locus for $P_{Ro\max}^*$ ($P_{Ro\max(1)}^*$, $P_{Ro\max(2)}^*$, $P_{Ro\max(3)}^*$)

Let us consider the last mode assuming that in low frequency mode the current advances generator voltage and in high frequency mode generator voltage advances the current. Analysis shows that in this case the same power value can be obtained by two operating modes with different M_q .

Indeed, the active power depends on u_{qo}^* by the following relation:

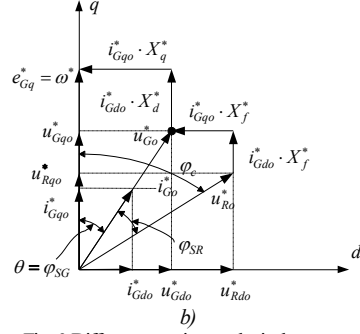
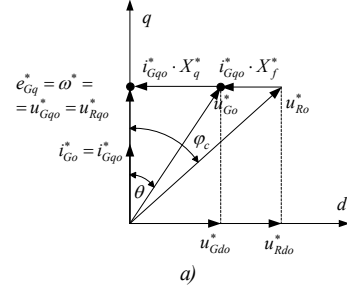


Fig. 6. Different operating modes in the system

$$\left[\frac{(P_{Ro}^* - P_0)}{\gamma_P R_{uP}} \right]^2 + \left[\frac{(u_{qo}^* - U_0)}{R_{uP}} \right]^2 = 1 \quad (7)$$

where

$$\gamma_P = \sqrt{\frac{k_L + q}{1 + q}}; \quad R_{uP} = \frac{\omega^*}{2} \sqrt{1 + \left(\operatorname{tg} \phi_{SG} / \sqrt{\frac{k_L + q}{1 + q}} \right)^2};$$

$$U_0 = \frac{\omega^*}{2}; \quad P_0 = \frac{\omega^*}{2} \cdot \operatorname{tg} \phi_{SG} / \left(\frac{k_L + q}{1 + q} \right).$$

From (7) we can obtain:

$$u_{qo1,2}^* = U_0 \mp \sqrt{-\left(\frac{P_{Ro}^* - P_0}{\gamma_P} \right)^2}; \quad u_{Ro}^* = \frac{k_L + q}{1 + q} P_{Ro}^*;$$

$$M_{q1,2} = \frac{2}{\sqrt{3}} u_{qo1,2}^*; \quad M_d = \frac{2}{\sqrt{3}} \frac{k_L + q}{1 + q} P_{Ro}^*.$$

It can be concluded from (8) and Fig. 6 that the same active power value can be obtain from two values of the voltage u_{Rqo}^* on the transverse axis, Fig. 7. In the relations (8) and further indexes 1 and 2 denote the operating modes 1 and 2 in accordance with Fig. 6.

Maximum power for certain frequency ω^* is defined from the following relation:

$$P_{Ro\max}^* = P_0 + \gamma_P R_{uP} \equiv \omega^* / 2 \quad (9)$$

Relations (8) make possible to obtain voltage dependences in the system as angular frequency functions with different values of ϕ_{SG} and parameters q and k_L .

The choice of an operating mode for the system as a WPI part will be considered further. Let us assume $q = 0$, $k_L = 1$ for the certainty. In this case equation (7) will be rewritten as:

$$\rho(\phi) = \omega^* \sec(\phi_{SG}) \sin(\phi + \phi_{SG})$$

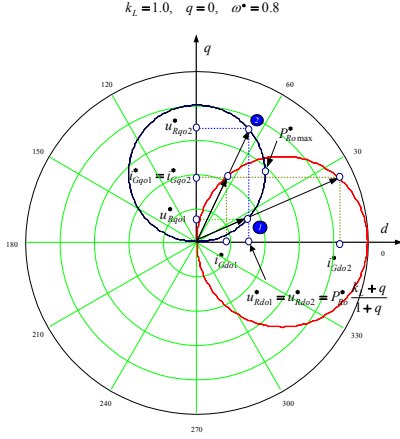


Fig. 7. First and second operating modes of the system

Besides, d - and q -components will be defined as:

$$\begin{aligned} P_{Ro}^*(\varphi) &= \omega^* \sec(\phi_{SG}) \sin(\phi + \phi_{SG}) \cos(\varphi); \\ u_{qo}^*(\varphi) &= \omega^* \sec(\phi_{SG}) \sin(\varphi + \phi_{SG}) \sin(\varphi). \end{aligned} \quad (10)$$

Fig. 8 shows proposed dependences of ϕ_{SG} and $\cos \phi_{SG}$ on the shaft angular frequency. This operating script makes possible to work with the second operating mode. Thereto match the system operating point for maximum WT power with maximum possible system power. Above and beyond it, maximum power P_{Ro}^* must be conformed to maximum modulation index $M = 1$, Fig. 9.

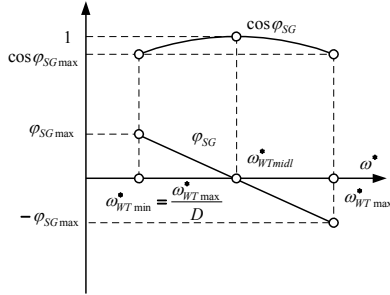


Fig. 8. Dependence of the angle between current and voltage in the generator

Let us denote $P_{Ro}^* = P_{Ro}^* \max \lim$. Angle φ_{\max} is defined from condition $d\rho(\varphi)/d\varphi = 0$ i.e. $\varphi_{\max} = \pi/4 - \phi_{SG}/2$. Rotating frequency for $P_{Ro}^* = P_{Ro}^* \max \lim$ can be found from the equation: $\rho(\varphi_{\max}) = \sqrt{3}/2$ hence:

$$\omega_{\max}^* = \frac{\sqrt{3}}{2} \cdot 1 / \sec(\varphi_{SG}) \cdot \sin\left(\frac{\pi}{4} + \frac{\varphi_{SG}}{2}\right)$$

As a result we obtain $P_{Ro}^* \max \lim = \frac{\sqrt{3}}{2} \cos\left(\frac{\pi}{4} - \frac{\phi_{SG}}{2}\right)$. Further,

let $\omega_{WT\max}^* = \omega_{\max}^*$; $P_{WTo}^* = P_{Ro}^* \max \lim$. From equation (4) we can obtain:

$$\gamma = P_{Ro}^* \max \lim / (\omega_{\max}^*)^3, \quad P_{WTo}^*(\omega^*) = P_{Ro}^* \max \lim \cdot (\omega^*)^3 / (\omega_{\max}^*)^3$$

In accordance with Fig. 9 let us assume $\phi_{SG} = -\phi_{SG\max}$ on condition $\omega^* = \omega_{\max}^*$. Also, the variation law of ϕ_{SG} within operating range $\omega^* \in \{\omega_{WT\min}^*, \omega_{WT\max}^*\}$ will be following:

$$\phi_{SG}(\omega^*) = \phi_{SG\max} [1 - 2 \cdot (\omega^* - \omega_{\min}^*) / (\omega_{\max}^* - \omega_{\min}^*)]$$

where $\omega_{\min}^* = \omega_{WT\min}^* = \frac{\omega_{WT\max}^*}{D_{WT}} = \frac{\omega_{\max}^*}{D_{WT}}$, $D_{WT} = \frac{\omega_{WT\max}^*}{\omega_{WT\min}^*}$.

Then

$$\omega_{\max}^* = \frac{\sqrt{3}}{2} \cdot 1 / \sec(\varphi_{SG}) \cdot \sin\left(\frac{\pi}{4} - \frac{\varphi_{SG\max}}{2}\right);$$

$$P_{Ro}^* \max \lim = \frac{\sqrt{3}}{2} \cos\left(\frac{\pi}{4} + \frac{\varphi_{SG\max}}{2}\right)$$

Minimum power with $\omega^* = \omega_{WT\min}^*$ will be

$$P_{Ro}^* \min = P_{Ro}^* \max \lim / (D_{WT})^3.$$

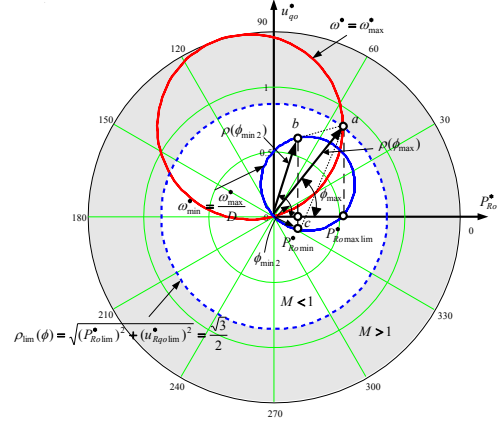


Fig. 9. Operating scripts of the system with varying ω^*

The locus for $\omega^* = \omega_{WT\min}^*$ is following:

$$\rho(\phi) = \omega_{WT\min}^* \sec(\varphi_{SG\max}) \sin(\phi + \varphi_{SG\max})$$

Angle $\varphi = \varphi_{\min}$ for that condition is found from the following equations:

$$\begin{aligned} \omega_{WT\min}^* \sec(\varphi_{SG\max}) \sin(\varphi_{\min} + \varphi_{SG\max}) \cos \varphi_{\min} &= P_{Ro}^* \max \lim / (D_{WT})^3 \\ \varphi_{\min 1} &= \frac{1}{2} \arcsin \left[2 \frac{P_{Ro}^* \max \lim}{D_{WT}^2 \omega_{WT\max}^* \sec(\varphi_{SG\max})} - \sin(\varphi_{SG\max}) \right] - \varphi_{SG\max}; \\ \varphi_{\min 2} &= \frac{\pi}{2} - (\varphi_{\min 1} + \varphi_{SG\max}). \end{aligned}$$

In these equations angles $\varphi_{\min 1}$ and $\varphi_{\min 2}$ are conformed to the operating modes 1 and 2 respectively.

There are two possible trajectories with varying frequency $\omega_{WT\min}^* \leftrightarrow \omega_{WT\max}^*$: $a \leftrightarrow c$ (in the first operating mode) and $a \leftrightarrow b$ (in the second operating mode).

Low power factor and high generator current are typical for the first operating mode. Therefore the second mode is more reasonable. Then:

$$M_d(\omega^*) = 2P_{WT_0}^*(\omega^*)/\sqrt{3};$$

$$M_q(\omega^*) = \omega^*/2 + \sqrt{(\omega^*/2)^2 - [P_{WT_0}^*(\omega^*)]^2 + \omega^* \text{tg}[\phi_{SG}(\omega^*)]P_{WT_0}^*(\omega^*)}.$$

For this case when $\phi_{SG \max} = \pi/12$ for $D_{WT} = 2$ on Fig. 11 calculation results of the current, voltage, power factor, active power and $\cos \phi_{SG}$ in dependence on $\omega^* \in \{\omega_{WT \min}^*, \omega_{WT \max}^*\}$ are presented.

It should be noticed that chosen linear variation law of $\phi_{SG}(\omega^*)$ is not only possible. In case of the prevalent wind velocity is known for given area, the shaft rotating frequency is calculated for this velocity on condition $\cos \phi_{SG} = 1$. In this case variation law of $\phi_{SG}(\omega^*)$ can be optimized an accordance with variation law of the wind velocity.

What is more, equality $\cos \phi_{SG} = 1$ in boundary values of operating range $\{\omega_{WT \min}^*, \omega_{WT \max}^*\}$ is not necessary.

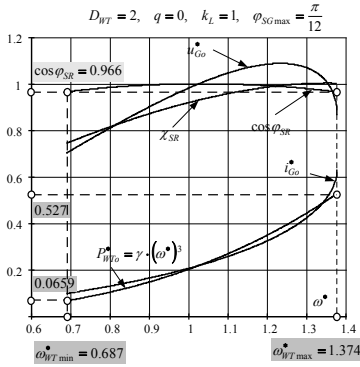


Fig. 10. System power characteristics

As can be seen from Fig. 11, this operating script choice makes possible to realize expanded operating range by increasing ω_{\max}^* for specified value of $\cos \phi_{SG}$. Dependence of $\phi_{SG \max}$ on specified angle value $\phi_{SG \max}$ is shown by Fig. 11. Figure also shows that maximum possible frequency is ω_{\max}^* for chosen operating script.

Thus, the operating script of the WPGS with varying $\cos \phi_{SG}$ by specified variation law in condition of varying ω_{WT}^* provides to increase maximum operating frequency and to save the second operating mode which has relatively high power factor.

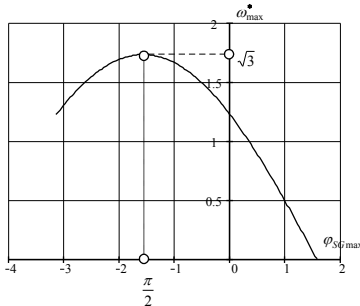


Fig. 11. Dependence of maximum operating frequency in the WPI on maximum angle between current and voltage in the generator.

III. MAIN POWER CHARACTERISTICS OF THE SYSTEM "VSI-ELECTRIC NETWORK"

Principle circuit of the system "Voltage Source Inverter – electric network" is given on Fig. 12.

Let us assume that variation law of the voltage in the electric network is following: $u_{N^*m} = U_{N^*} \cos[\nu - (m-1)2\pi/3]$, where $\nu = \Omega t$, $m = 1, 2, 3$ ($u \ v \ w$).

Besides, inverter control signals are defined by the equation: $u_{i_{cm}} = u_c \cos(\theta_m)$, where $\theta_m = \nu - (m-1)2\pi/3 + \phi_{ic}$. The following quantities have been chosen as basic frequency and resistance: $\omega_{\delta} = \Omega$, $X_{\delta} = \omega_{\delta} L_j$. Let us introduce the term of the frequency ratio: $a_1 = \omega_{cl}/\Omega$, where ω_{cl} – is the angular PWM frequency and Ω – angular frequency of electric network. One more assumption is $U_{dc} = \sqrt{3} \cdot U_{N^*} \cdot \delta_{U_{dc}}$, where $\delta_{U_{dc}} \geq 1$ is exceeding of the minimum possible dc-link voltage.

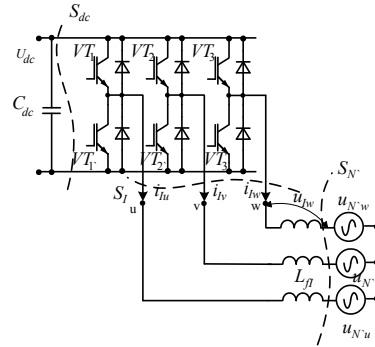


Fig. 12. Principle circuit of the system "Voltage Source Inverter – electric network"

Taking into account all above mentioned assumptions and denoted quantities a mathematical model of the circuit in the dq -frame can be presented as:

$$u_{id}^* = di_{id}^*/d\nu - i_{iq}^*, \quad u_{iq}^* - 1 = di_{iq}^*/d\nu + i_{id}^*, \quad (11)$$

where $\nu = \Omega t$. In (11) Electric network voltage is oriented by q axis.

Voltages u_{id}^* and u_{iq}^* can be defined by the following equations:

$$u_{id}^* = u_{ido}^* + \Delta u_{id}^*;$$

$$u_{iq}^* = u_{iqo}^* + \Delta u_{iq}^*;$$

$$u_{ido}^* = \delta_{U_{dc}} M \sqrt{3}/2 \cdot \sin(-\phi_{Rc}) = -\delta_{U_{dc}} M_d \sqrt{3}/2;$$

$$u_{iqo}^* = \delta_{U_{dc}} M \sqrt{3}/2 \cdot \cos(-\phi_{Rc}) = \delta_{U_{dc}} M_q \sqrt{3}/2;$$

Here u_{ido}^* , u_{iqo}^* – are d and q components of the fundamental harmonic of the inverter output voltage; Δu_{id}^* , Δu_{iq}^* – are d and q components of the higher harmonic of the inverter output voltage.

Higher harmonics for SPWM are defined by the equation (3) with taking into account coefficient $\delta_{U_{dc}}$.

In steady state condition analytical equations for inverter currents can be defined through the equations (3), (11) and (12). In this

case d and q components of the fundamental harmonic are defined as $i_{lqo}^* = -u_{ldo}^*$; $i_{ld}^* = u_{lqo}^* - 1$.

Let us consider the control algorithm of the inverter when WPI generates into the electric network active power only. With this algorithm $u_{lqo}^* = 1$; $i_{lo}^* = i_{lqo}^* = -u_{ldo}^*$; $i_{ld}^* = 0$ and generated active power is defined by the following equation:

$$P_{No}^* = i_{lqo}^* = i_{lo}^* = -u_{ldo}^* \quad (13)$$

D and q components of the inverter control signals and angle ϕ_{lc} are defined as: $M_q = 2/(\sqrt{3} \cdot \delta_{Udc})$, $M_d = 2 \cdot P_{No}^* / (\sqrt{3} \cdot \delta_{Udc})$, $\phi_k = \arctg M_d / M_q = \arctg P_{No}^*$.

Linear working range of the inverter is limited by the following condition:

$$\begin{aligned} \sqrt{(M_d)^2 + (M_q)^2} &\leq \left\{ 1 - SPWM, 2/\sqrt{3} - SVPWM; \right. \\ \frac{2}{\sqrt{3}} \cdot \frac{1}{\delta_{Udc}} \sqrt{1 + (P_{No}^*)^2} &\leq \left\{ 1 - SPWM, 2/\sqrt{3} - SVPWM, \right. \end{aligned} \quad (14)$$

From this equation (in case of equality) we can obtain equation for the maximum active power which can be transferred into the network without current distortion:

$$P_{No \max}^* = \begin{cases} \sqrt{(\sqrt{3}/2 \cdot \delta_{Udc})^2 - 1}, & -SPWM \\ \sqrt{(\delta_{Udc})^2 - 1}, & -SVPWM. \end{cases} \quad (15)$$

From (15) follows that the minimum value of $\delta_{Udc \min}$ for generating active power is defined by the equation:

$$\delta_{Udc \min} = \begin{cases} 2/\sqrt{3} - SPWM; \\ 1 - SVPWM. \end{cases}$$

Dependence of the active power P_{No}^* on $\delta_{Udc} = U_{dc} / \sqrt{3} U_N$ and on modulation index can be found through this equation:

$P_{No}^* = \sqrt{(\sqrt{3} \delta_{Udc} M / 2)^2 - 1}$. With taking into account active losses at the output of the WPI the fundamental harmonic of the current will be following:

$$i_{lo}^* = P_{No}^* = \frac{1}{1 + (\omega_R^*)^2} \cdot \left\{ \sqrt{[1 + (\omega_R^*)^2] \left(\frac{2}{\sqrt{3} \delta_{Udc} M} \right)^2 - 1} - \omega_R^* \right\};$$

where $\omega_R^* = R / X_{\sigma} R$ - equivalent active inverter phase resistance.

The plot of $P_{No}^*(M)$ for SV PWM is shown on Fig. 13. It can be seen from Fig. 13 that regulating range decreases if δ_{Udc} decreases. It should be noticed that using of SV PWM provides significantly increasing generated active power. Fig. 14 also shows that for each value of δ_{Udc} there is a minimum modulation index M_{\min} . If the modulation index less than $M_{\min} = 2/(\sqrt{3} \delta_{Udc})$ the active power is zero.

Dependence of inverter current THD on the WT shaft frequency will be defined further.

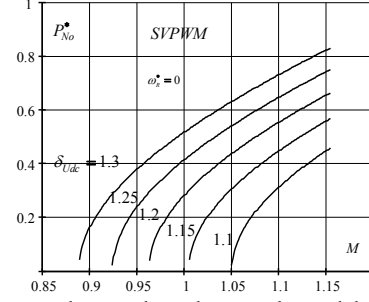


Fig. 13. Generated power dependence on the modulation index.

In accordance with (13) and results obtained in [2], RMS values of the fundamental harmonic of current $i_{lo, rms}^*$, ripple component $\Delta i_{l, rms}^*$ and total RMS value of the inverter current are defined by the following equations:

$$\begin{aligned} i_{lo, rms}^* &= \frac{1}{\sqrt{2}} P_{No}^*, \\ \Delta i_{l, rms}^* &= \left(\frac{\sqrt{3} \delta_{Udc}}{\pi \cdot X_{\Sigma}^*} \right) \cdot \left(J_1(\pi \cdot M)^2 \frac{a_l^2 + 1}{(a_l + 1)^2 (a_l - 1)^2} \right)^{\frac{1}{2}}, \\ i_{l, rms}^* &= \sqrt{(i_{lo, rms}^*)^2 + (\Delta i_{l, rms}^*)^2}. \end{aligned}$$

Modulation index depends on the WT shaft frequency as follows (in accordance with the condition (15)):

$$M = 2 \cdot \sqrt{\left[P_{No \max}^* \cdot \left(\omega / \omega_{WT \max} \right)^3 \right]^2 + 1} / \sqrt{3} \delta_{Udc}.$$

Knowing of this dependence can be used to find power characteristics of the generated power as functions of WT shaft frequency. As an example Fig. 14 shows plots of $THD_{il}(\omega / \omega_{WT \max})$ for SV PWM.

Since in high power WPI frequency ratio a_l is limited by the dynamic losses in switches, it can be concluded that it is impossible to meet the power quality demands by increasing PWM frequency without LC filter. Increasing of δ_{Udc} causes increasing of the dc-link voltage and, as a consequence, rated power of the inverter.

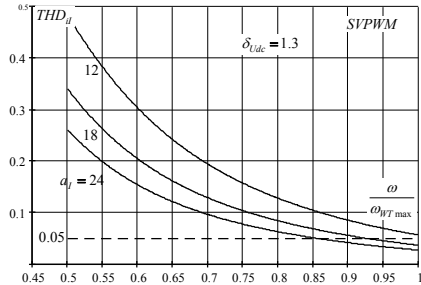


Fig. 14. THD of the generator current in dependence on WT angular frequency.

Changing of the inverter topology or decreasing of the regulating range of power with SVPWM can solve this problem. Therefore design of WPI with rated power 1MW or more must be oriented to multilevel inverter topologies.

Another solution is parallel connection of m inverters. All inverters are connected to the same dc voltage source and controlled by the same control signal in each phase, but switching times in every inverter are delayed by angle $2\pi/m$ in relative to each other. It can be realized, for example, by introducing m control signals with specified phase delay. This solution increases power of the system above and beyond energy quality performance. It also provides modular construction for such systems. Advantage of modular construction is saving the same efficiency of the system with low and high WT shaft frequency. This feature is provided by different numbers of modules. Number of the modules is a function of the shaft frequency.

Increasing of channels number causes excluding groups of mixed harmonics from the current spectrum with the following harmonic orders: $\nu = n \cdot \omega_{kl} \pm p \cdot \Omega$; $n < m$. Calculation shows that decreasing of the current THD can be evaluated by this equation: $THD_{il(m)} \approx THD_{il(1)} / m^2$, where $THD_{il(1)}$ – is the total harmonic distortion with $m=1$.

Besides that, number of mixed harmonics groups is also decreases in the amplitude-frequency spectrum of the current in dc-link i_{dc} . Power factor $\chi_{Sdc(m)}$ in section S_{dc} , Fig. 12, in the inverters' inputs can be evaluated by the following equation [4]:

$$\chi_{Sdc(m)} = \left[\sqrt{1 + \frac{1 - (\chi_{Sdc(1)})^2}{(\chi_{Sdc(1)})^2} \cdot \frac{1}{m^2}} \right]^{-1},$$

where $\chi_{Sdc(1)}$, $\chi_{Sdc(m)}$ – are power factors in section S_{dc} for single channel and m channels respectively.

It can be concluded that parallel inverter connection causes increasing of the generated power by m times, decreasing THD about m^2 times. What is more, for the same frequency ratio a_b , reactive power density of the dc-link capacitor C_{dc} decreases m times. On the other hand, for the same THD using of parallel inverter connection provides to decrease frequency ratio m^2 times.

Thus, performed analysis of the system "VSI – Electric network" makes possible to evaluate main power characteristics of the system analytically in different operating conditions and control algorithms. In conditions of low wind velocity THD of the system does not meet the demands of power quality when WPI works for high power networks. This problem is solved by using of multilevel converters, applying SVPWM control, modular inverter topology. Latest solution increases the efficiency of WPGS by disabling of several channels when low shaft frequency. Modular construction principle can be applied in WPGS. Fig. 15 shows an example of modular-based WPGS.

Fig. 16 shows dependence of the power in a generating module of WPGS in different intervals of the shaft frequency variation.

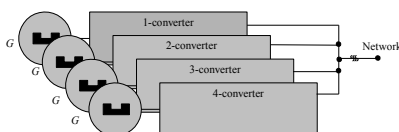


Fig. 15. Modular construction principle in WPGS

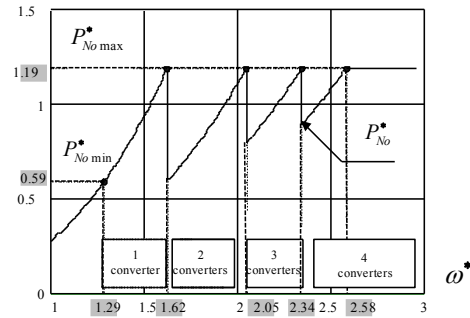


Fig. 16. Dependence of the power in a generating module of WPGS

It can be seen that first one module works, then two modules, after – three etc. Increasing number of the modules decreases rated range of each module and increases system efficiency in condition of low wind velocity. Besides that maximum power of the system increases and its power quality still high. Using this technology a WPI named "Raduga" was designed and built near Elista city. WPI has rated power 1MW and consists of four modules. Each module includes permanent magnet synchronous generator, frequency converter, control system and matching transformer. Operating wind velocity range: 4–25m/s.

CONCLUSIONS

A mathematical model for analysis of power characteristics of the system including permanent magnet synchronous generator, active rectifier and voltage source inverter has been considered.

A control algorithm for the active rectifier and inverter with taking into account variable wind turbine shaft has been considered.

Analytical equations for generated power and its different graphic dependences on different parameters and operation modes were presented.

Useful recommendations for choosing control algorithms and structures of WPI considering variable wind turbine were formulated.

ACKNOWLEDGMENT

The authors would like to thank the Ministry of Knowledge and Economy which partly supported this research through the Network-based Automation Research Center (NARC) at the University of Ulsan.

REFERENCES

- [1] Z. Chen, J. M. Guerrero, and F. Blandjerg "A Review of State of the Art of Power Electronics for Wind Turbines" *IEEE Trans. on Power Electronics*, vol. 24, NO. 8, August 2009, pp. 1659 – 1875.
- [2] Kharitonov S.A. "The power system "permanent magnet synchronous generator - active rectifier". (Mathematical model)", *Elekrotehnika. M. 2009, №12, p. 33-41.*
- [3] Com G., Com T. "Mathematics handbook (for science officers and engineers)". - *M. - the Science, 1974. in Russian*
- [4] Kharitonov S.A. "Integrated parameters and characteristics of voltage inverters in structure of generating systems of an alternating current such as "variable speed - constant frequency" for wind-energetic installations", *Scientific bulletin NSTU, Novosibirsk, 1999. pp. 92 – 120, in Russian.*